Association between Carbonyl Sulfide Uptake and $^{18}\Delta$ during Gas Exchange in C_3 and C_4 Leaves[1][OA]

Keren Stimler, Joseph A. Berry, Steve A. Montzka, and Dan Yakir*

Environmental Sciences and Energy Research, The Weizmann Institute of Science, Rehovot 76100, Israel (K.S., D.Y.); Department of Global Ecology, Carnegie Institution of Washington, Stanford, California 94305 (J.A.B.); and National Oceanic and Atmospheric Administration Earth System Research Laboratory, Boulder, Colorado 80305 (S.A.M.)

Carbonyl sulfide (COS) and $C^{18}OO$ exchange by leaves provide potentially powerful tracers of biosphere-atmosphere CO_2 exchange, and both are assumed to depend on carbonic anhydrase (CA) activity and conductance along the diffusive pathway in leaves. We investigated these links using C_3 and C_4 plants, hypothesizing that the rates of COS and $C^{18}OO$ exchange by leaves respond in parallel to environmental and biological drivers. Using CA-deficient antisense lines of C_4 and C_3 plants, COS uptake was essentially eliminated and discrimination against $C^{18}OO$ exchange ($^{18}\Delta$) greatly reduced, demonstrating CA's key role in both processes. $^{18}\Delta$ showed a positive linear correlation with leaf relative uptake (LRU; ratio of COS to CO_2 assimilation rates, A^s/A^c, normalized to their respective ambient concentrations), which reflected the effects of stomatal conductance on both COS and $C^{18}OO$ exchange. Unexpectedly, a decoupling between A^s and $^{18}\Delta$ was observed in comparing C_4 and C_3 plants, with a large decrease in $^{18}\Delta$ but no parallel reduction in A^s in the former. This could be explained by C_4 plants having higher COS concentrations at the CA site (maintaining high A^s with reduced CA) and a high phospho*enol*pyruvate carboxylase/CA activity ratio (reducing ^{18}O exchange efficiency between CO_2 and water, but not A^s). Similar A^s but higher A^c in C_4 versus C_3 plants resulted in lower LRU values in the former (1.16 ± 0.20 and 1.82 ± 0.18 for C_4 and C_3, respectively). LRU was, however, relatively constant in both plant types across a wide range of conditions, except low light (<191 μmol photon m^{-2} s^{-1}).

The seasonal cycling of CO_2 concentration measured in the background atmosphere is often taken as evidence of the breathing of Earth and corresponds to about 10 Pg carbon. This is less than 10% of what we estimate to be the total cycling of CO_2 due to respiration and photosynthesis of the terrestrial biosphere (Beer et al., 2010). The discrepancy stems from the fact that most of the cycling CO_2 mixes in the atmosphere near the surface, and we only see the net sum of respiration and photosynthesis, which are often more or less balanced over the seasonal cycle. Modeling and measurements of CO_2 exchange by ecosystems over diurnal cycles have been used to deconvolve the primary biological processes (e.g. Desai et al., 2008). However, our confidence in these approaches disintegrates as we move to larger scales because of the increase in the internal mixing of CO_2 fluxes. Other approaches are needed to quantify the basic physiological processes at these scales.

Recent studies have identified another atmospheric trace gas that may be helpful in this regard—carbonyl sulfide (COS)—a chemical analog of CO_2 that is routinely measured by the National Oceanic and Atmospheric Administration atmospheric sampling program (Montzka et al., 2007). However, its cycling differs from that of CO_2. The major source of COS is the ocean either by direct emission or via CS_2 oxidation (Kettle et al., 2002), and its major sink is the leaves of the terrestrial biosphere, where it is taken up in parallel with photosynthesis. There is no significant source of COS from terrestrial ecosystems; hence, the mixing between sources and sinks occurs on a much larger scale in the atmosphere. Several authors have suggested that COS might be a good tracer for terrestrial gross primary productivity (GPP; Montzka et al., 2007; Blake et al., 2008; Campbell et al., 2008; Suntharalingam et al., 2008; Seibt et al., 2010). The initial development of this tracer was built on theoretical insight into the likely mechanism of COS uptake and a few empirical studies that compared the rates of GPP and COS uptake at the leaf scale (Sandoval-Soto et al., 2005). However, if the goal is to use COS exchange estimates as a proxy for gross photosynthesis (or GPP) on larger scales, then it becomes important to understand the physiological basis for linking these fluxes.

At the leaf scale, correlations of both COS and CO_2 fluxes with photosynthetically active radiation have been interpreted as evidence of stomata-dominated control of COS uptake rates, an interpretation that is supported by the daily pattern of this flux (Bartell

[1] This work was supported by the Israel Science Foundation, the U.S.-Israel Binational Science Foundation, and the Minerva Foundation.

* Corresponding author; e-mail dan.yakir@weizmann.ac.il.

The author responsible for distribution of materials integral to the findings presented in this article in accordance with the policy described in the Instructions for Authors (www.plantphysiol.org) is: Dan Yakir (dan.yakir@weizmann.ac.il).

[OA] Open Access articles can be viewed online without a subscription.

www.plantphysiol.org/cgi/doi/10.1104/pp.111.176578

et al., 1993; Hofman, 1993; Kuhn et al., 1999; Xu et al., 2002). Stimler et al. (2010a) also recently confirmed that there is no leaf-scale compensation point for COS, supporting the notion of no COS emission on this scale. The deposition velocity (flux normalized to concentration) for COS has been shown to be greater than that for CO_2 in most species, with a mean ratio of the deposition velocities of COS to CO_2 at the leaf level of about 3 (Sandoval-Soto et al., 2005). Recently, Campbell et al. (2008) expressed these ratios as leaf-scale relative uptake (LRU):

$$\mathrm{LRU} = (A^s/A^c)\times(C_a^c/C_a^s) \quad (1)$$

where A is the leaf uptake rate, C_a is the ambient concentration, and superscript s and c denote COS and CO_2, respectively. As clearly revealed by Campbell et al. (2008), characterizing LRU and its response to environmental and physiological drivers is key to incorporating COS measurements into flux-partitioning studies.

In vitro studies have established that COS, which is meta stable in water, can be hydrolyzed to H_2S and CO_2 by the enzyme carbonic anhydrase (CA; Kluczewski et al., 1985; Lorimer and Pierce, 1989; Miller et al., 1989; Tiwari et al., 2005; see also Yakir, 2002). This enzyme is ubiquitous in plant leaves and is thought to be the biochemical sink for COS, which is further enhanced as this is an exergonic reaction, making the reverse reaction unfavorable (Liu et al., 2010):

$$H_2O + COS \overset{CA}{\rightarrow} CO_2 + H_2S \quad (2)$$

This enzyme is also known to catalyze the exchange of stable isotopes of oxygen between CO_2 and leaf water. This isotopic exchange can be monitored by measuring the change in the ^{18}O content of CO_2 in gas exchange as well as in large-scale flux studies (Farquhar et al., 1993; Yakir and Wang, 1996; Gillon and Yakir, 2001). For CO_2, CA facilitates the reversible hydration (Lindskog and Coleman, 1973):

$$H_2O + CO_2 \overset{CA}{\leftrightarrow} H^+ + HCO_3^- \quad (3)$$

This reversible hydration/dehydration of CO_2 provides the opportunity for efficient ^{18}O exchange between leaf water, normally enriched in ^{18}O, and CO_2 inside the leaf (Francey and Tans, 1987; Farquhar and Lloyd, 1993; Farquhar et al., 1993; Yakir and Wang, 1996; Gillon and Yakir, 2000, 2001; Seibt et al., 2007).

$C^{18}O^{16}O$ isotopic exchange and COS flux can be expected to respond to the same variables. Sufficient CA activity is needed to both bring about full isotopic equilibrium and maintain near-zero COS concentration at the site of CA activity. Furthermore, the same diffusion resistances limit both the inward diffusion of COS flux into leaves and the retrodiffusion of ^{18}O-labeled CO_2 back into the atmosphere. Note, however, that the diffusion gradient of CO_2 is driven by the photosynthetic flux, while that of COS is independent of it.

Recognizing the potential importance of incorporating COS into gas exchange and flux measurements, we developed a laser-based instrument for the continuous measurement of COS concentration at normal atmospheric levels (approximately 400 parts per trillion, or one-millionth the concentration of CO_2). This instrument enables conducting gas exchange studies analogous to those typically conducted with nondispersive infrared gas analyzers (Stimler et al., 2010a). A subsequent study (Stimler et al., 2010b) examined the stoichiometry of COS and CO_2 fluxes in leaves of C_3 and C_4 species with particular emphasis on the control of these processes by stomatal conductance (g_s). In this article, we focus on the mechanism of COS uptake. We also hypothesize that COS uptake will be closely linked to ^{18}O labeling of CO_2 during leaf gas exchange, and we take advantage of natural and genetically engineered variations in CA to examine this hypothesis.

RESULTS AND DISCUSSION

Relative COS/CO_2 Uptake in C_3 versus C_4 Plants

The mean rates of net CO_2 assimilation (A^c) and COS uptake (A^s) and the fluxes involved are summarized in Table I and Figure 1, respectively, and are consistent with previous studies (Kesselmeier and Merk, 1993; Sandoval-Soto et al., 2005; Stimler et al., 2010a). Due to the higher A^c but similar A^s values for C_4 compared to C_3 plants, the LRU values were higher in the latter (Table I; Fig. 2; see Kesselmeier and Merk, 1993; Sandoval-Soto et al., 2005; Seibt et al., 2010; Stimler et al., 2010a). Irrespective of these differences, the results showed that, as noted previously for C_3 plants (Stimler et al., 2010a), LRU is relatively constant across a wide range of light intensities in both C_3 and C_4 plants. Large deviations were only observed under low light (<191 μmol photon m^{-2} s^{-1}), when the ratio could increase to up to 9.6 in both C_3 and C_4 plants (Fig. 2B). These results support the assumption that both A^c and A^s are influenced to a similar extent by stomatal conductance. Indeed, A^s was linearly correlated to g_s ($A^s = 322.0g_s + 11.2$; $r^2 = 0.78$, $P < 0.0001$ for C_3, and $A^s = 109.0g_s + 3.4$; $r^2 = 0.86$, $P < 0.0001$ for C_4). The deviations from the relatively constant LRU under low light probably reflect the light dependency of Rubisco activation and of ribulose 1,5-bisP supply, whereas CA activity is presumably light insensitive (Sage and Sharkey, 1987).

Stomatal conductance is only one of the two major factors regulating leaf COS exchange. Ultimately, COS uptake depends on the reaction rate of COS with CA and water to produce CO_2 and H_2S (Eq. 2; Liu et al., 2010; Stimler et al., 2010a). Here, we confirmed the critical role of CA by carrying out light response experiments with CA-deficient antisense lines of C_3 and C_4 species (Price et al., 1994; von Caemmerer et al., 2004). COS uptake was essentially eliminated in both

Table I. *COS versus CO_2 uptake fluxes; simple (A^s/A^c) or normalized (LRU = $A^s/A^c \times ([CO_2]/[COS])$) ratio of COS and CO_2 uptake rates, and COS total conductance under maximum-intensity light, for C_4 and C_3 plants*

Gas exchange conditions during the light response experiments were T approximately 24°C, RH approximately 70%, [COS] approximately 550 pmol mol^{-1}, and $[CO_2]$ = 400 μmol mol^{-1}; two to five replicates per species; SD is indicated in parentheses.

Plant Species	A^s/A^c	LRU	A^s	A^c	g_t^s
	$\mu mol\ mol^{-1}$		$pmol\ m^{-2}\ s^{-1}$	$\mu mol\ m^{-2}\ s^{-1}$	$mol\ m^{-2}\ s^{-1}$
C_4					
Maize	1.97 (0.50)	1.05 (0.76)	42.33 (3.65)	16.23 (5.04)	0.17 (0.18)
Sorghum	1.91 (0.39)	1.05 (0.44)	34.10 (13.91)	20.20 (4.18)	0.09 (0.06)
Amaranthus	2.51 (0.85)	1.37 (0.79)	41.54 (10.38)	17.48 (3.72)	0.13 (0.04)
Average	2.13 (0.33)	1.16 (0.18)	39.32 (4.54)	17.97 (2.03)	0.13 (0.04)
C_3					
Tobacco	2.61 (0.96)	1.63 (0.36)	27.01 (4.89)	9.41 (2.08)	0.1 (0.03)
Sage	2.67 (1.11)	1.82 (0.89)	40.80 (24.38)	13.50 (5.71)	0.05 (0.03)
Hibiscus	2.87 (1.28)	2.02 (0.29)	40.23 (12.68)	9.91 (1.25)	0.07 (0.02)
Average	2.72 (0.14)	1.82 (0.20)	36.01 (13.98)	10.94 (3.01)	0.07 (0.03)

of these antisense lines (Fig. 3). In the C_3 plants, this was not associated with significant changes in g_s or A^c (Fig. 3, A, C, and E). In C_4 plants, however, antisense lines also showed reductions in A^c and g_s (Fig. 3, B, D, and F). This presumably reflects the C_4 pathway's dependence on bicarbonate, produced by the CA-facilitated hydration of CO_2.

Note that in this study, the use of CA-deficient antisense lines did not address the entire range of CA types or enzyme locations in the plants' leaves (Fabre et al., 2007). Nevertheless, the CA that was affected in these lines clearly dominated the COS and ^{18}O response.

COS Exchange and $^{18}\Delta$

Consistent with previous studies (Farquhar and Lloyd, 1993; Gillon and Yakir, 2001), leaf-scale discrimination against $C^{18}OO$ ($^{18}\Delta$) was correlated with C_{cs}/C_a in all plants (Fig. 4D; where C_{cs} refers to CO_2 concentration at the chloroplast surface). Moreover, the C_4 plants showed markedly lower $^{18}\Delta$ than the C_3 plants. This most likely reflects incomplete isotopic equilibrium between CO_2 and water in the C_4 leaves, and accounting for this effect (i.e. $\theta_{eq} < 1$; Gillon and Yakir, 2000, 2001) revealed consistent relationships between $^{18}\Delta$ and C_{cs}/C_a in both C_4 and C_3 plants (Fig. 4).

As expected (see above; see also Stimler et al., 2010a), a clear negative correlation was observed between A^s and $^{18}\Delta$. This correlation was apparent in all leaves during the light response experiments, for both C_4 and C_3 species (Fig. 4A, showing representative species). Increasing light intensity was generally associated with a decrease in $^{18}\Delta$ values and increases in A^s. For example, A^s increased from 15 to 43 pmol m^{-2} s^{-1} and from 8 to 24 pmol m^{-2} s^{-1}, whereas $^{18}\Delta$ decreased from 84‰ to 13‰ and from 48‰ to 12‰ in amaranthus (*Amaranthus cruentus*) and sorghum (*Sorghum halepense*), respectively. In C_3 species, A^s increased from 20 to 46 pmol m^{-2} s^{-1} and from 20 to 35 pmol m^{-2} s^{-1}, while $^{18}\Delta$ values decreased from 157‰ to 40‰ and from 239‰ to 81‰, for sage (*Salvia longispicata* × *Salvia farinacea*) and tobacco (*Nicotiana tabacum*), respectively. This inverse correlation between A^s and $^{18}\Delta$ is readily explained by the effects of g_s and C_{cs}: Increasing g_s with light intensity results in increasing uptake rates of COS (as well as CO_2). At the same time, the increase in photosynthetic capacity with increasing light intensity leads to a decrease in C_{cs}, resulting in decreased retroflux of ^{18}O-labeled CO_2 out of the leaf and, consequently, in the observed reduction in $^{18}\Delta$ (see Farquhar and Lloyd, 1993; Gillon and Yakir, 2001).

On average, a reduction of 75‰ in $^{18}\Delta$ was associated with a decrease in C_{cs}/C_a, from 0.7 to 0.4, in C_3 plants and from 0.5 to 0.2 in C_4 plants. As the decrease in C_{cs} reflects a proportionately greater increase in photosynthetic capacity (influencing only A^c and not A^s) relative to stomatal conductance (but g_s influences both A^c and A^s), it can be expected that the LRU will also change under these circumstances. Indeed, linear relationships between LRU and $^{18}\Delta$ were observed (r^2 = 0.76, 0.87, and 0.99) for the C_4 species sugarcane (*Saccharum officinarum*), sorghum, and maize (*Zea mays*), and r^2 = 0.89, 0.98, and 0.79 for the C_3 species hibiscus (*Rosa sinensis*), tobacco, and sage, respectively. Grouping the results for the C_4 and C_3 plants yielded best-fit lines of $y = 0.51x - 4.58$ with $r^2 = 0.78$ ($P < 0.0001$) for C_4 plants and $y = 0.03x - 0.20$ with $r^2 = 0.92$ ($P < 0.0001$) for C_3 plants.

The COS-$^{18}\Delta$ Link in C_4 versus C_3 Plants

The correlation between LRU and $^{18}\Delta$ covered the entire range of both wild-type and CA-deficient antisense lines of C_3 plants (Fig. 5A), but not of C_4 plants (Fig. 5B), or in comparing C_3 to C_4 plants (Fig. 6). Unexpectedly, while $^{18}\Delta$ was lower in C_4 than in C_3 plants, consistent with previous studies (Gillon and Yakir, 2000, 2001), there was essentially no difference

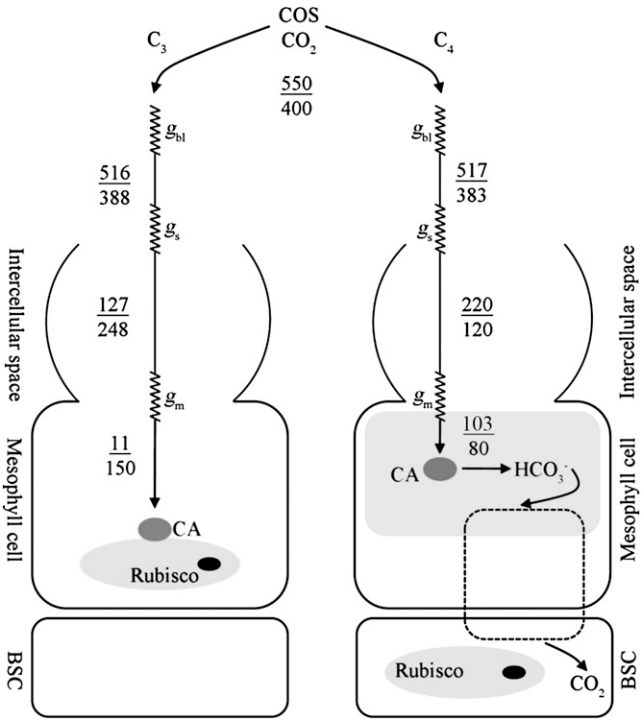

Figure 1. Comparison of the diffusion pathways of COS and CO_2 from the atmosphere to the site of biochemical reactions in C_3 and C_4 leaves. Concentrations of COS (pmol mol^{-1}) and CO_2 (μmol mol^{-1}) are indicated above and below the lines, respectively. Conductance through resistance steps associated with the boundary layer, stomata, and mesophyll (mol m^{-2} s^{-1}) are indicated by g_{bl}, g_s, and g_m, respectively, based on leaves with net CO_2 flux of 14 or 20 μmol m^{-2} s^{-1} (C_3 and C_4, respectively), and COS uptake flux of approximately 35 pmol m^{-2} s^{-1} (for both plant types). Values of g_m (0.3 mol m^{-2} s^{-1} for both C_4 and C_3 leaves, respectively) were estimated by Stimler et al. (2010a) and incorporate dissolution, liquid-phase diffusion, and the biochemical step (assuming first-order reaction); g_m estimates for CO_2 were based on CO_2 concentration at the hydration site derived from isotopic measurements (Gillon and Yakir, 2001).

in the rate of COS uptake between the two photosynthetic groups (mean A^s values of 36.0 ± 13.9 and 39.32 ± 4.54 pmol m^{-2} s^{-1} for C_3 and C_4, respectively). Other variables generally showed the expected differences between C_3 and C_4 leaves: A^c was markedly higher, C_i/C_a (CO_2) lower, and g_s (CO_2) similar in C_4 compared to C_3 leaves (Fig. 6; Table I). C_i^s/C_a^s (for COS) was <0.2, as observed previously in C_3 plants (Stimler et al., 2010a), but twice as high in C_4 plants (Fig. 6D), which may reflect differences in internal resistances, as well as the fact that CA is located higher up (toward the atmosphere) in the diffusive pathway in C_4 versus C_3 leaves (see Fig. 1).

The explanation for the unexpected discrepancy between changes in $^{18}\Delta$ and A^s in going from C_3 to C_4 plants can be based on two mechanisms. These mechanisms are outlined below, but at this stage we do not have sufficient information to accurately quantify their relative contributions.

First, note that as indicated above, low $^{18}\Delta$ values for C_4 plants result from incomplete isotopic equilibrium between CO_2 and water (Gillon and Yakir, 2000; Eq. 3), which is assumed to be due to reduced CA activity (observed in whole-leaf extracts of C_4 leaves; Gillon and Yakir, 2000). No parallel reduction in COS flux was observed in the C_4 plants examined (Fig. 6B), indicating sufficient CA activity. Note that in going from C_3 to C_4 plants, g_s remains similar but C_i/C_a (CO_2) decreases and C_i^s/C_a^s (COS) increases. This is likely because a reduction in C_i^c (CO_2) in C_4 leaves is associated with higher A^c, whereas an increase in C_i^s (COS) is associated with lower CA activity. The increase in C_i^s (COS),

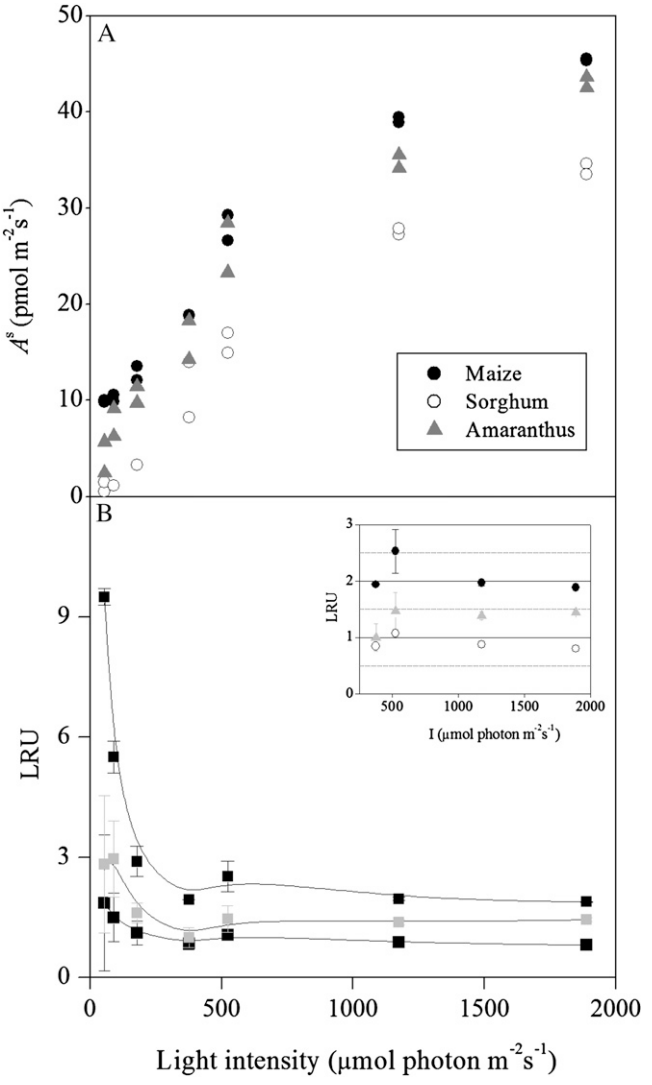

Figure 2. COS uptake rates (pmol m^{-2} s^{-1}; A) and LRU values (B) during light response measurements in C_4 plants. Species used were: maize, sorghum, and amaranthus. Conditions during the experiments were: T approximately 24°C, RH approximately 70%, [COS] approximately 550 pmol mol^{-1}, and [CO_2] = 400 μmol mol^{-1}. Symbols without error bars have SD < 2% (in section B only). Inset: LRU (the normalized ratio of COS/CO_2 uptake rates) under high light intensity.

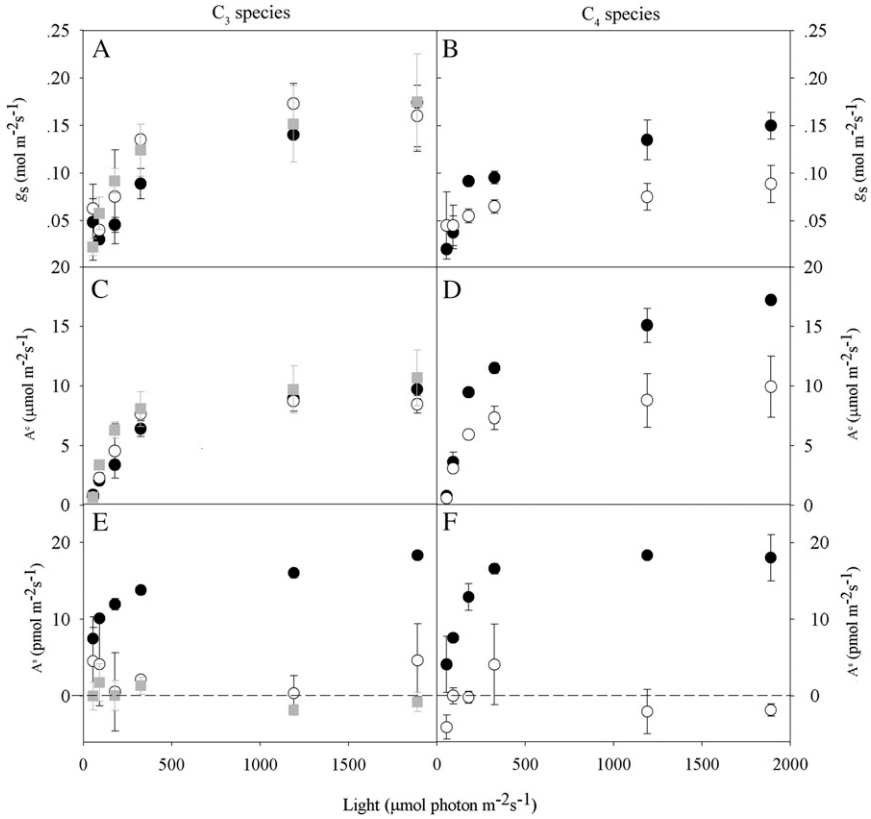

Figure 3. Stomatal conductance (g_s; mol m^{-2} s^{-1}; A and B), CO_2 uptake (A^c; μmol m^{-2} s^{-1}; C and D), and COS uptake (A^s; pmol m^{-2} s^{-1}; E and F) in tobacco (C_3) and *F. bidentis* (C_4) wild-type and antisense lines with different levels of CA activity during the light response experiments. Conditions during the experiments were as in Figure 2. Symbols (black circles, white circles, and gray squares) indicate wild type, moderate (10%, C_3 and C_4 plants), and low (2%, C_3 only) CA activities of the antisense lines, respectively.

however, helps restore A^s to levels similar to those in C_3 plants. Therefore, given that A^s is a function of both CA and the COS concentration at the enzyme site, the higher C_i^s/C_a^s observed in the C_4 plants (Fig. 6D) could accommodate proportionately lower CA activity while maintaining relatively high A^s values. This could explain, at least in part, the observed discrepancy in A^s versus $^{18}\Delta$. Accordingly, estimating total internal conductance to COS, g^s_m (combining dissolution and the biochemical steps, assuming a first-order reaction, as: $g_m{}^s = 1/[(C_a{}^s/A^s) - (1/(1.94/g_s{}^w) + 1/(1.56/g_{bl}{}^w))]$; see Stimler et al., 2010a), indicated a mean $g_m{}^s$ value of

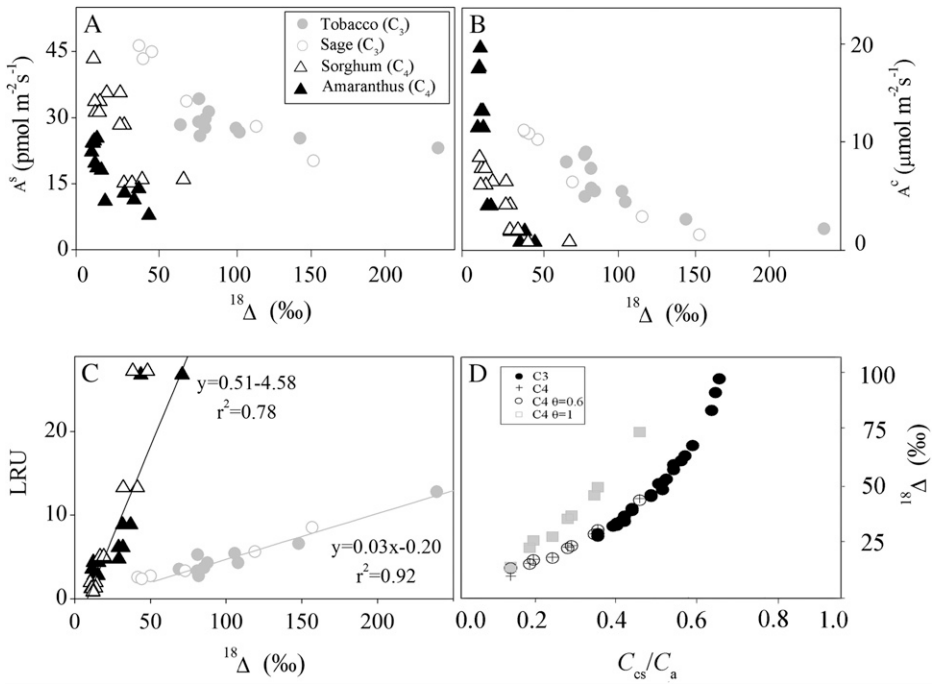

Figure 4. Relationships between $C^{18}OO$ ($^{18}\Delta$; ‰) and rates of COS uptake (pmol m^{-2} s^{-1}; A), CO_2 uptake (μmol m^{-2} s^{-1}; B), and LRU (C), observed in C_3 (circles) and C_4 (triangles) plants. Each curve represents the full set of data from a complete light response experiment. In C, r^2 values for the linear best-fit lines for C_4 and C_3 plants are indicated ($P < 0.0001$). D, The relationship between $^{18}\Delta$ and CO_2 concentrations at the hydration site (C_{cs}) from different light response experiments and plants. Conditions during gas exchange measurements were as in Figure 2. Black circles and crosses represent observed discrimination values; white symbols represent predicted values based on the indicated parameters and as described in Table II, following Gillon and Yakir (2001).

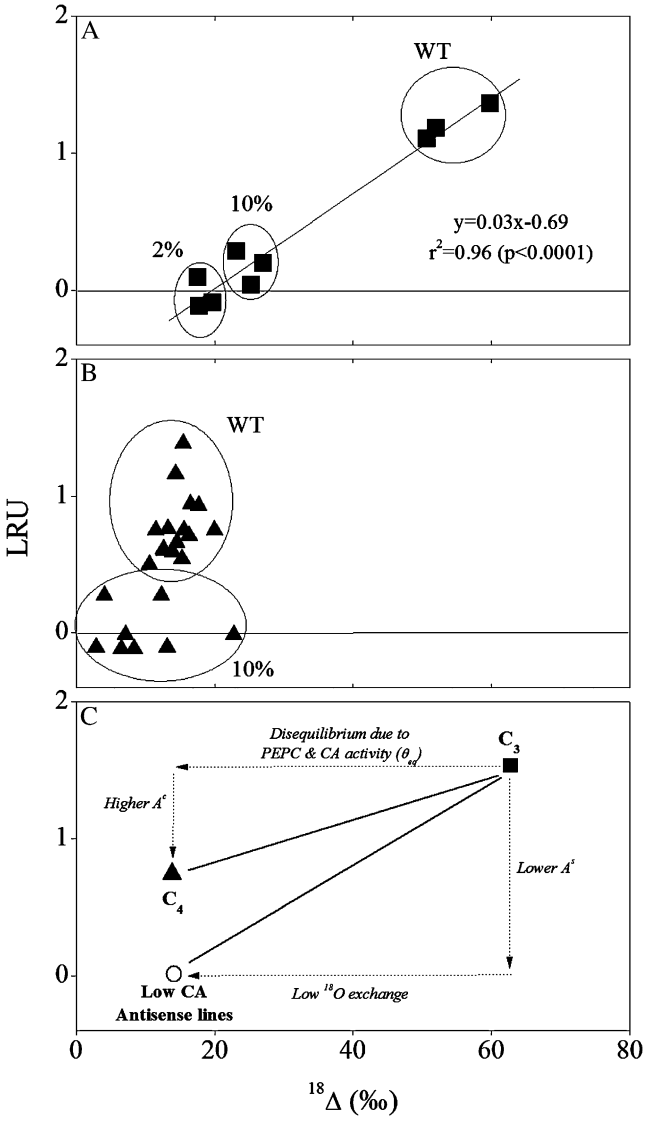

Figure 5. Relationship between LRU and ^{18}O discrimination ($^{18}\Delta$) in plants with different levels of CA activity (antisense lines). A, Mean values in C_3 species (tobacco) with moderate and low levels of CA activity (percent of wild type). B, Data of C_4 species (*F. bidentis*) with moderate CA activity. Values are based on light response experiments under high light intensity (1,889 μmol photon m^{-2} s^{-1}) and all other conditions as in Figure 2. C, Schematic summary of the relationships between LRU and $^{18}\Delta$ values, indicating the possible factors underlying the observed changes based on data from A and B. CA deficiency eliminates COS uptake (LRU approaches zero) and reduces ^{18}O discrimination ($^{18}\Delta$) in both C_3 and C_4 plants. Compared to C_3 wild-type plants, the C_4 wild-type (WT) species show a small decrease in LRU (lower A^s/A^c due to high A^c values in these plants) but a large decrease in $^{18}\Delta$ (PEPC in these plants limits ^{18}O exchange and CO_2-water isotopic equilibrium).

approximately 0.3 mol m^{-2} s^{-1} similar to our earlier study and, considering the observed variations (about $\pm$0.5), similar for both C_3 and C_4 plants. This upholds the high internal COS concentration near the biochemical reaction site (Fig. 1).

The second mechanism that could help explain the A^s versus $^{18}\Delta$ discrepancy (required when, for example, the reduced CA activity accommodated by the first mechanism remains too high to produce previously reported θ_{eq} values) relies on the fact that in C_4 plants, the primary photosynthetic substrate is bicarbonate consumed by phospho*enol*pyruvate carboxylase (PEPC; Cousins et al., 2007). A high ratio of PEPC to CA activity, ρ, must result in reduced bicarbonate concentrations which, in turn, reduce the efficiency of the isotopic exchange between CO_2 and water (the ratio of Rubisco to CA activities is assumed to be low and is neglected here; see Farquhar and Lloyd, 1993). Since PEPC activity directly influences the hydration rate, the apparent CO_2 hydration rate constant, K_H, should not be identical to the CA rate constant, CA_{leaf}, originally used in estimating θ_{eq} (Gillon and Yakir, 2001). To account for this effect, we revised the disequilibrium term introduced in Gillon and Yakir (2001), substituting K_H for CA_{leaf}, where $K_H = CA_{leaf} \times (1 - \rho)$, to obtain:

$$\theta_{eq} = 1 - e^{-(K_H/F_{in}/3)} = 1 - e^{-\left(CA_{leaf}(1-\rho)/F_{in}/3\right)} \quad (4)$$

where CA_{leaf} is the hydration rate scaled to leaf conditions ($CA_{leaf} = k/F_{in}$, k is CA rate constant, F_{in} is the gross CO_2 influx rate, μmol m^{-2} s^{-1}), and 3 reflects the slower isotopic exchange associated with the three oxygens in bicarbonate.

Limited information is available on the variations in PEPC and CA activities among plant species. Based on our gas exchange data, supplemented with values in the literature (e.g. Cousins et al., 2007), we can assume for a typical C_4 leaf, with A^s of approximately 40 pmol m^{-2} s^{-1} and C_i^s/C_a^s of approximately 0.4, midrange CA activity of approximately 600 μmol m^{-2} s^{-1} and PEPC activity of approximately 100 μmol m^{-2} s^{-1}, which yields ρ = 0.17. This, in turn, results in a disequilibrium, θ_{eq}, value of approximately 0.7, consistent with the observed mean value of approximately 0.6 (Fig. 4D) for our C_4 plants. As expected, θ_{eq} values approach zero and 1 when ρ values approach 1 and zero, respectively. Note that the above estimates of the ρ effects incorporate both the effect of the relatively high PEPC activities and the high C_i^s in C_4 leaves.

Similar effects of PEPC on $^{18}\Delta$ have been demonstrated previously using amaranthus (C_4) plants with different levels of PEPC (Cousins et al., 2007). In that study, suppressing the enzyme activity by a factor of approximately 40 enhanced $^{18}\Delta$ from 16.8‰ to 207‰, consistent with our results, but this was ascribed to errors in estimating CA activities. Note that in C_4 plants, there was no change in $^{18}\Delta$ between the wild-type and antisense lines (Fig. 5B), which may indicate similar CA/PEPC in both plants or an effect on $^{18}\Delta$ of CA/PEPC in the wild type similar to the reduced CA in the antisense plants.

Our current, preliminary, perspective of the links between COS uptake rates and $^{18}\Delta$, summarized in Figure 5C, highlights three points. First, $^{18}\Delta$ in C_4 plants is

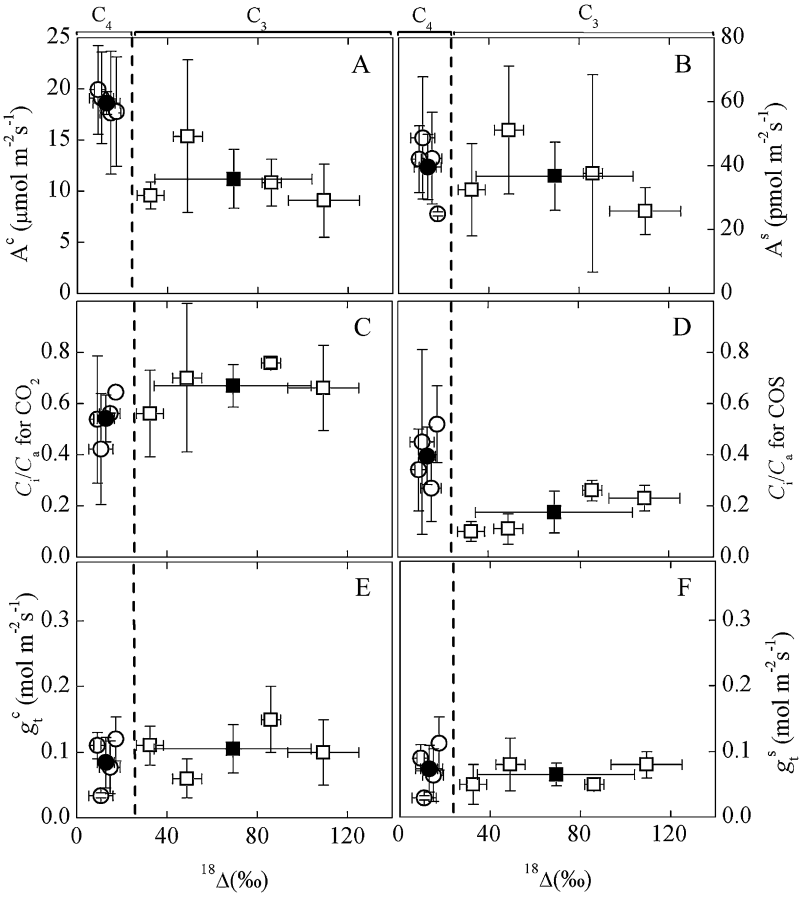

Figure 6. Relationships between gas exchange parameters and ^{18}O discrimination ($^{18}\Delta$) in C_3 and C_4 plants. A and B, Rates of CO_2 uptake (A^c; A) or COS uptake (A^s; B); C and D, ratio of intercellular to ambient concentrations of CO_2 (C_i^c/C_a^c; C) and COS (C_i^s/C_a^s; D); E and F, total leaf conductance of CO_2 (g_t^c; E) or COS (g_t^s; F). Data are compiled from different light response experiments with C_4 (circles) and C_3 (squares) species. Each data point represents four to six measurements (SD is indicated). Black symbols indicate mean values. C_4 species used were maize, sorghum, and amaranthus, and C_3 species were sage, tobacco, and hibiscus.

markedly reduced compared to C_3 plants, as has been repeatedly reported. Second, CA activity is key to both ^{18}O discrimination and COS uptake. Third, $^{18}\Delta$ and LRU are decoupled in C_4 plants because of the high C_i^s and reduced bicarbonate concentrations associated with high PEPC activity.

CONCLUSION

In this study, we extend our previous results showing that LRU is relatively constant in both C_3 and C_4 plants. We show that the two processes, COS uptake and $C^{18}OO$ exchange, can be measured simultaneously and that their rates are closely correlated, whether modulated by changing environmental conditions or by manipulating the activity of the key enzyme CA. The unexpected decoupling of COS and $C^{18}OO$ exchange in comparing C_3 and C_4 plants demonstrated that our understanding of CA reaction and ^{18}O discrimination in leaves is incomplete. Both COS and C^{18} can serve as potentially powerful tracers of plant-atmosphere CO_2 fluxes, and as a means to partition these fluxes to their gross components. Using the observed links between COS and $^{18}\Delta$ could greatly improve their use as tracers and constrain interpretations of the underlying processes.

Table II. *Isotopic and gas exchange values for a C_4 plant (amaranthus) based on light response measurements (compare, Fig. 4D)*

$^{18}\Delta^m$ and $^{18}\Delta^p$ are measured and predicted ^{18}O discrimination (‰) when $\theta_{eq} = 1$ and $\theta_{eq} = 0.6$ (full or partial isotopic equilibrium, respectively), $\varepsilon = C_{cs}/(C_a - C_{cs})$ where C_a and C_{cs} indicate ambient and chloroplast surface CO_2 concentrations, Δ_{ea} is isotopic discrimination between atmospheric CO_2, δ_a, and that in equilibrium with leaf water, δ_e: $\Delta_{ea} = 1{,}000 \times [(\delta_e/1{,}000 + 1)/(\delta_a/1{,}000 + 1) - 1]$. Irradiance values are in μmol photon m^{-2} s^{-1}. Analysis and definitions are based on Gillon and Yakir (2001).

Irradiance	$^{18}\Delta^m$	$^{18}\Delta^p$ ($\theta_{eq} = 0.6$)	$^{18}\Delta^p$ ($\theta_{eq} = 1$)	ε	Δ_{ea}
171	30.2	30.35	48.87	0.95	35.55
352	31.1	31.58	51.10	1.00	31.25
524	23.35	23.62	36.93	0.72	31.30
1,179	16.95	17.26	25.54	0.45	32.78
1,889	3.77	10.20	14.20	0.18	34.59

MATERIALS AND METHODS

Plant Material

C_3 species sage (*Salvia longispicata* × *Salvia farinacea*), tobacco (*Nicotiana tabacum*), and hibiscus (*Rosa sinensis*) were purchased from local nurseries. C_4 species maize (*Zea mays*) and sorghum (*Sorghum halepense*) were grown from seeds in the greenhouse, while amaranthus (*Amaranthus cruentus*) and sugarcane (*Saccharum officinarum*) were purchased from nurseries. CA-deficient antisense line and wild-type seeds of tobacco (C_3) and *Flaveria bidentis* (C_4) were contributed by Prof. S. von Caemmerer (Australian National University) and grown in the greenhouse. Various levels of CA activity were achieved using the suppression methods described by Price et al. (1994) and von Caemmerer et al. (2004). Plants were kept under ambient light and temperature during the experimental period.

Gas Exchange Measurements

Uptake rates of CO_2 and COS were measured in all C_3 and C_4 plants with attached leaves. The experimental system consisted of a flow-through leaf cuvette made of Teflon-coated stainless steel with a magnetically operated fan and a glass window at the top. A whole leaf or branch was sealed in the cuvette (O-ring seal except around the petiole, which was sealed with high-vacuum putty). Measurements were performed under a relative humidity (RH) of approximately 70% and an air temperature of approximately 24°C. Light intensity was 55 to 1,889 μmol photon m^{-2} s^{-1}, regulated with layers of miracloth, and filtered through 5 cm of water. Continuous airflow coming out of the cuvette was split into two paths for COS and CO_2 analysis. Following the CO_2 analysis, the sampled air was passed through a magnesium perchlorate drying trap (Sigma-Aldrich) to remove water before collecting the air in 115-mL flasks for analysis of the isotopic composition of CO_2. COS and CO_2 mixing ratios in air entering the leaf cuvette were adjusted to the desired values by mixing purified synthetic air with known gas mixtures produced from a COS-permeation device (VICI Metronics), and a compressed gas mixture of 1% CO_2 in air, followed by a three-stage dilution system. All flow rates were regulated and measured by mass-flow controllers (MKS).

CO_2 and COS Analyses

CO_2 and water-vapor concentrations in the air entering and leaving the leaf cuvette were measured by an infrared gas analyzer (Li-6262; Li-Cor) at a precision better than 0.5 μmol mol^{-1} for CO_2 and 0.1 mmol mol^{-1} for water vapor.

COS concentrations were measured using a mid-IR dual quantum cascade laser spectrometer (Aerodyne Research Inc.) at a wavenumber of 2,056 cm^{-1} with a LN_2-cooled HgCdTe (MCT) detector (Kolmar Technologies) as described by Stimler et al. (2010b). Briefly, direct detection of the absorption spectrum was followed by quantitative spectral fitting combined with the measured pressure, temperature, and path length of the absorption cell and the laser spectral line width using TDL WINTEL software, as described by Nelson et al. (2004). The concentrations of COS and the laser line widths were determined in real time from the spectra through a nonlinear least-squares fitting algorithm that uses spectral parameters from HITRAN (Rothman et al., 2003). The data analysis procedure included pulse normalization reduction of the sample signal and automatic background correction (N_2). Pulse normalization corrects for variations in pulse-to-pulse amplitude in pulsed laser systems, by normalizing the signal pulse train to a reference pulse train. The automatic background correction divides the sample spectra by the spectrum of dry N_2. Corrections were carried out every 300 s.

Isotopic Analysis of CO_2

Oxygen isotope analysis of CO_2 was based on sampling CO_2 in the air entering and exiting the leaf cuvette by passing it through a 115-mL glass flask under atmospheric pressure. The CO_2 in the flask was measured as described by Klein et al. (2005). Briefly, a 1.5-mL aliquot was removed from each flask into a sampling loop and the CO_2 was cryogenically trapped using helium as the carrier gas. It was then passed through a Carbosieve G-packed column at 70°C to separate N_2O, and the eluted CO_2 was analyzed in a Europa 20-20 continuous-flow isotope ratio mass spectrometer (Crewe). Batches of 15 flasks at a time were measured from an automated manifold system, with five flasks of a standard gas being measured for every 10 samples at a precision of 0.2‰. Results are expressed in the small δ notation (δ‰) versus VPDB-CO_2 for ^{18}O, where $\delta‰ = (R_{sample}/R_{standard} - 1) \times 1{,}000$ and R_{sample} and $R_{standard}$ are the isotopic ratios of the sample and the appropriate standard, respectively. Instantaneous leaf discriminations, Δ, were calculated as described by Evans et al. (1986) for ^{13}C and extended to ^{18}O (Gillon and Yakir, 2001). The isotopic composition of CO_2 in air supplied to the leaves during the experiments was around $\delta^{18}O = -27‰$. The $\delta^{18}O$ values of water supplied to the plants was −5‰, and that of leaf water at the evaporating surfaces was estimated using the modified Craig-Gordon model (Craig and Gordon, 1965; Farquhar and Lloyd, 1993) to be 10‰ ± 2‰ (depending on conditions and species).

Leaf discrimination against $C^{18}OO$, $^{18}\Delta$, and the extent of CO_2-water isotopic equilibrium, θ_{eq}, were calculated as detailed by Farquhar and Lloyd (1993) and Gillon and Yakir (2000). Calculation of CO_2 concentration at the hydration site (C_{cs}) was based on the difference between the measured and predicted discrimination against ^{13}C ($^{13}\Delta$) as described by Gillon and Yakir (2000), based on the approach of Evans et al. (1986). For $^{18}\Delta$ estimation in C_4 plants, incomplete isotopic equilibrium (θ_{eq}) was assumed, as measured by Gillon and Yakir (2001).

Received March 17, 2011; accepted June 27, 2011; published June 29, 2011.

LITERATURE CITED

Bartell U, Hoffman U, Hoffman R, Kreuzburg B, Andreae MO (1993) OCS and H_2S fluxes over a wet meadow in relation to photosynthetic activity: an analysis of measurements made on 6th September 1990. Atmos Environ **27A:** 1851–1864

Beer C, Reichstein M, Tomelleri E, Ciais P, Jung M, Carvalhais N, Rödenbeck C, Arain MA, Baldocchi D, Bonan GB, et al (2010) Terrestrial gross carbon dioxide uptake: global distribution and covariation with climate. Science **329:** 834–838

Blake NJ, Campbell JE, Vay SA, Fuelberg HE, Huey LG, Sachse G, Meinardi S, Rowland FS, Blake DR (2008) Carbonyl sulfide (OCS): large scale distributions over North America during INTEX-NA and relationship to CO_2. J Geophys Res **113:** D09S90

Campbell JE, Carmichael GR, Chai T, Mena-Carrasco M, Tang Y, Blake DR, Blake NJ, Vay SA, Collatz GJ, Baker I, et al (2008) Photosynthetic control of atmospheric carbonyl sulfide during the growing season. Science **322:** 1085–1088

Cousins AB, Baroli I, Badger MR, Ivakov A, Lea PJ, Leegood RC, von Caemmerer S (2007) The role of phosphoenolpyruvate carboxylase during C_4 photosynthetic isotope exchange and stomatal conductance. Plant Physiol **145:** 1006–1017

Craig H, Gordon HI (1965) Deuterium and oxygen-18 variations in the ocean and marine atmosphere. *In* E Tongiorgi, ed, Proceedings of a Conference on Stable Isotopes in Oceanographic Studies and Palaeotemperatures. Laboratory of Geology and Nuclear Science, Pisa, Italy, pp 9–130

Desai AR, Richardson AD, Moffat AM, Kattge J, Hollinger DY, Barr A, Falge E, Noormets A, Papale D, Reichstein M, et al (2008) Cross-site evaluation of eddy covariance GPP and RE decomposition techniques. Agric Forest Meteorol **148:** 821–838

Evans JR, Sharkey TD, Berry AJ, Farquhar GD (1986) Carbon isotope discrimination measured concurrently with gas exchange to investigate CO_2 diffusion in leaves of higher plants. Aust J Plant Physiol **13:** 281–292

Fabre N, Reiter IM, Becuwe-Linka N, Genty B, Rumeau D (2007) Characterization and expression analysis of genes encoding alpha and beta carbonic anhydrases in Arabidopsis. Plant Cell Environ **30:** 617–629

Farquhar GD, Lloyd J (1993) Carbon and oxygen isotope effects in the exchange of carbon dioxide between terrestrial plants and the atmosphere. *In* JR Ehleringer, AE Hall, GD Farquhar, eds, Stable Isotopes and Plant Carbon-Water Relations. Academic Press, San Diego, pp 47–70

Farquhar GD, Lloyd J, Taylor JA, Flanagan AB, Syverts JP, Hubick KT, Wong SC, Ehleringer JR (1993) Vegetation effects on the oxygen isotopic composition of atmospheric CO2. Nature **363:** 439–443

Francey RJ, Tans PP (1987) Latitudinal variation in oxygen-18 of atmospheric CO_2. Nature **327:** 495–497

Gillon JS, Yakir D (2001) Influence of carbonic anhydrase activity in terrestrial vegetation on the ^{18}O content of atmospheric CO_2. Science **291:** 2584–2587

Gillon JS, Yakir D (2000) Naturally low carbonic anhydrase activity in C_4

and C_3 plants limits discrimination against $C^{18}OO$ during photosynthesis. Plant Cell Environ **23:** 903–915

Hofman DJ (1993) 20 years of balloon-borne trophospheric aerosol measurements at Laramie, Wyoming. J Geophys Res-Atmos **98:** 12753–12766

Kesselmeier J, Merk L (1993) Exchange of carbonyl sulfide (COS) between agricultural plants and the atmosphere: studies on the deposition of COS to peas, corn and rapeseeds. Biogeochemistry **23:** 47–59

Kettle AJ, Kuhn U, von Hobe M, Kesselmeier J, Andreae MO (2002) Global budget of atmospheric carbonyl sulfide: temporal and spatial variations of the dominant sources and sinks. J Geophys Res **107:** 4658

Klein T, Hemming D, Lin T, Grünzweig JM, Maseyk K, Rotenberg E, Yakir D (2005) Association between tree-ring and needle $\delta^{13}C$ and leaf gas exchange in Pinus halepensis under semi-arid conditions. Oecologia **144:** 45–54

Kluczewski SM, Brown KW, Bell JNB (1985) Deposition of [^{35}S]-carbonyl sulphide to vegetable crops. Radiat Prot Dosimetry **11:** 173–177

Kuhn U, Ammann C, Wolf A, Meixner FX, Andreae MO, Kesselmeier J (1999) OCS exchange on an ecosystemscale: soil represents a dominant sink for atmospheric OCS. Atmos Environ **33:** 995–1008

Lindskog S, Coleman JE (1973) Catalytic mechanism of carbonic anhydrase. Proc Natl Acad Sci USA **70:** 2505–2508

Liu Y, Ma J, He H (2010) Heterogeneous reactions of carbonyl sulfide on mineral oxides: mechanism and kinetics study. Atmos Chem Phys **10:** 10335–10344

Lorimer GH, Pierce J (1989) Carbonyl sulfide: an alternate substrate for but not an activator of ribulose-1,5-bisphosphate carboxylase. J Biol Chem **264:** 2764–2772

Miller AG, Espie GS, Canvin DT (1989) Use of carbon oxysulfide, a structural analog of CO_2, to study active CO_2, transport in the Cyanobacterium synechococcus UTEX 625. Plant Physiol **90:** 1221–1231

Montzka S, Calvert P, Hall BD, Elkins JW, Conway TJ, Tans PP, Sweeny C (2007) On the global distribution, seasonality and budget of atmospheric carbonyl sulfide (COS) and some similarities to CO2. J Geophys Res **112:** D09302

Nelson DD, McManus B, Urbanski S, Herndon S, Zahniser MS (2004) High precision measurements of atmospheric nitrous oxide and methane using thermoelectrically cooled mid-infrared quantum cascade lasers and detectors. Spectrochim Acta A Mol Biomol Spectrosc **60:** 3325–3335

Price GD, von Caemmerer S, Evans JR, Yu JW, Lloyd J, Oja V, Kell P, Harrison K, Gallagher A, Badger MR (1994) Specific reduction of chloroplast carbonic anhydrase activity by antisense RNA in transgenic tobacco plants has a minor effect on photosynthetic CO_2 assimilation. Planta **193:** 331–340

Rothman LS, Barbe A, Benner DC, Brown LR, Camy-Peyret C, Carleer MR, Chance K, Clerbaux C, Dana V, Devi VM, et al (2003) The HITRAN molecular spectroscopic database: edition of 2000 including updates through 2001. J Quant Spectrosc Radiat Transfer **82:** 5–44

Sage RF, Sharkey TD (1987) The effect of temperature on the occurrence of O_2 and CO_2 insensitive photosynthesis in field grown plants. Plant Physiol **84:** 658–664

Sandoval-Soto L, Stanimirov M, von Hobe M, Schmitt V, Valdes J, Wild A, Kesselmeier J (2005) Global uptake of carbonyl sulfide (COS) by terrestrial vegetation: estimates corrected by deposition velocities normalized to the uptake of carbon dioxide (CO2). Biogeosciences **2:** 125–132

Seibt U, Kesselmeier J, Sandoval-Soto L, Kuhn U, Berry JA (2010) A kinetic analysis of leaf uptake of COS and its relation to transpiration, photosynthesis and carbon isotope fractionation. Biogeosciences **7:** 333–341

Seibt U, Wingate L, Berry JA (2007) Nocturnal stomatal conductance effects on the delta(18)O signatures of foliage gas exchange observed in two forest ecosystems. Tree Physiol **27:** 585–595

Stimler K, Montzka SA, Berry JA, Rudich Y, Yakir D (2010a) Relationships between carbonyl sulfide (COS) and CO_2 during leaf gas exchange. New Phytol **186:** 869–878

Stimler K, Nelson D, Yakir D (2010b) High precision measurements of atmospheric concentrations and plant exchange rates of carbonyl sulfide (COS) using mid-IR Quantum Cascade Laser. Glob Change Biol **16:** 2496–2503

Suntharalingam P, Kettle AJ, Montzka S, Jacob DJ (2008) Global 3-D model analysis of the seasonal cycle of atmospheric carbonyl sulfide: implications for terrestrial vegetation uptake. Geophys Res Lett **35:** L19801

Tiwari A, Kumar P, Singh S, Ansari SA (2005) Carbonic anhydrase in relation to higher plants. Photosynthetica **43:** 1–11

von Caemmerer S, Quinn V, Hancock NC, Price GD, Furbank RT, Ludwig M (2004) Carbonic anhydrase and C_4 photosynthesis: a transgenic analysis. Plant Cell Environ **27:** 697–703

Xu X, Bingemer HG, Schmidt U (2002) The flux of carbonyl sulfide and carbon disulfide between the atmosphere and a spruce forest. Atmos Chem Phys **2:** 171–181

Yakir D (2002) Global enzymes: sphere of influence. Nature **416:** 795

Yakir D, Wang XF (1996) Fluxes of CO_2 and water fluxes between terrestrial vegetation and the atmosphere estimated from isotope measurements. Nature **380:** 515–517